

Efficiency Improvement of WRIM Using DSP Controller By Adding Rotor Capacitance

¹D. Muralidharan.,²P. Anitha Rani,³R. Aswani

¹ Assistant Professor, Department of Electrical and Electronics Engineering
V.S.B Engineering College, Karur-639111, Tamilnadu, India

^{2,3}P.G Scholar, Power Systems Engineering,
V.S.B College of Engineering, Karur -639111, Tamilnadu, India

Abstract— The paper presents a novel secondary reactance control technique in the rotor circuit of a three phase wound rotor induction motor (WRIM). The problem associated with the conventional rotor capacitive reactance control is the demand of exceptionally large capacitance requirement for enhancing the performance of the motor in wide operating range. In the proposed technique, a three phase bridge rectifier with a dynamic capacitor is used in the rotor circuit. The dynamic capacitor is H-bridge circuit with a capacitor in which the duty cycle of switching elements is varied for emulating the capacitance value dynamically and to be used as capacitive reactance control. A TMS320F2407 Digital Signal Processor (DSP) controller is used for delivering Pulse Width Modulation (PWM) pulses for appropriate switches. The performances such as speed, torque, power factor, efficiency, harmonics of the motor are analyzed for different speed and loading conditions. The feasibility of the proposed system is verified by simulation and experimental results.

Keywords: *Wound Rotor Induction Motor (WRIM), DSP Controller, Dynamic Capacitor (DC), Secondary Reactance Control, Rotor Capacitive Reactance Control (RCRC), Pulse Width Modulation (PWM).*

1. INTRODUCTION

It is known from the literature and energy saving points that more than 60% of total electrical energy consumed worldwide is by Induction motors. Although Induction motors, specifically, squirrel cage types are widely used in electrical drives, wound rotor induction motor (WRIM) has some distinct applications like high torque, starting with high inertia loads, adjustable speed drives and soft starts. Hence the utility of wound rotor induction motor has also been

increased on par with squirrel cage types of motors. In recent years, more attention has been given for efficiency and power factor improvement of these motors for significantly saving electrical energy. Several methods have been proposed for performance improvement of WRIM by rotor control. These can be distinctively classified as rotor resistance control and rotor impedance control. In rotor resistance control, if equal resistances are included in each secondary phase of three phase induction motor, the speed, starting current and torque can be controlled. However speed decreases as the secondary resistances increase. At the same time, if the rotor circuit is added with additional resistances, the losses increase which in turn decrease the efficiency of the motor. There are a number of chopper controlled rotor resistance control methods which have been presented and their performance were analyzed in [1]-[5].

In order to overcome the problem faced by rotor resistance control, instead of varying the rotor resistance alone, the rotor impedance variation and control have been proposed in the literature to control the speed, torque and performance of the motor in [6]-[11]. A novel method for controlling the speed of WRIM by operating such a motor close to its resonance has been introduced in [12]. In this method, the induction motor produces maximum torque when the rotor resistance is approximately equal to the slip times of the rotor reactance. In order to get the resonant condition, a capacitive reactance has been introduced in the rotor circuit for cancelling the inductive reactance of the rotor circuit. Speed control of an induction motor is possible by having a resonant rotor circuit, which is adjusted according to the slip frequency. The main drawback of this method is the requirement of high value of capacitance (order of Farad) required to operate the machine close to rotor resonance conditions.

In order to overcome the problem faced in [12], a switched capacitor concept has been adopted for the secondary control of an induction motor to improve the efficiency, power factor and torque in [13]. It utilizes the concept of switched capacitor [14] which makes use of four thyristors as switches to form H-bridge circuit and a single capacitor in the middle of the H-Bridge which are connected in each rotor phase. The complementary switch pairs are switched using a PWM strategy. This paper describes the improvement of various performance parameters and speed control of the wound rotor induction machine. The main drawback of this method is that the speed is varied by varying the duty cycle of four fast acting switches (IGBT) and eight fast recovery diodes for each phase of the rotor circuit. Additionally, this technique requires three capacitors suitable for continuous motor operation.

Another technique [16], in which the speed control of WRIM is obtained using chopper controlled external resistance enhanced with a dc capacitor. The efficiency of motor is significantly reduced due to the external rotor resistor control. The double capacitor, double switch switched capacitance topology were proposed in [19] in which the range of capacitance value that can be varied is between the two capacitor's capacitance values.

This paper addresses a novel method to overcome losses due to rotor resistance control and dynamically controlling the performances of the motor. To solve this problem, the present technique introduces a dynamic capacitor in the rotor circuit as shown in Fig.1 Since the rotor employs bridge rectifier circuit, the induction motor secondary windings can be operated at any induced voltage and variable frequency with respect to different slip conditions. The performance of the motor such as power factor, efficiency, speed, torque and the order of harmonics are measured. The experimental and simulation results as function at different load and varies emulated rotor capacitor conditions are analyzed and presented in this paper.

2. MODELING OF THE INDUCTION MOTOR WITH ROTOR CAPACITIVE REACTANCE CIRCUIT

For the theoretical analysis, the following assumptions, regarding the induction motor, are made.

1) That the stator and rotor are cylindrical with a Smooth air gap and symmetrical three-phase windings displaced by 120 electrical degrees.

2) That the magnetic circuit is assumed to be infinitely permeable with a radial flux density in the air gap.

3) The effect of iron losses and end-effects are neglected.

The equivalent circuit of the WRIM with rotor capacitive reactance circuit is shown in the Fig. 2.

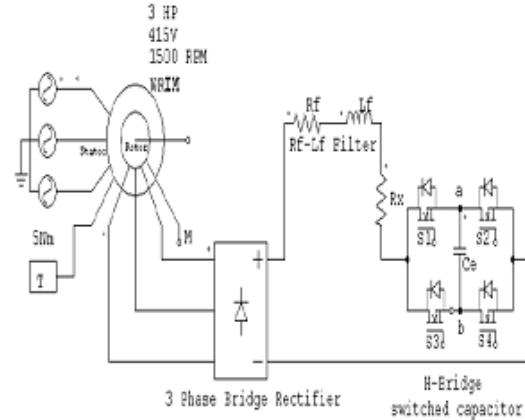


Figure.1 Power Circuit of Proposed Control Scheme

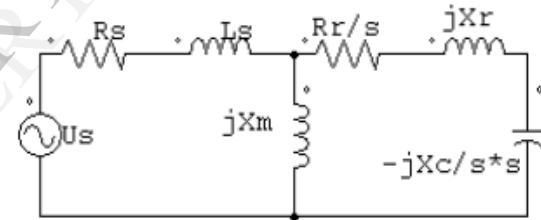


Figure 2. Equivalent circuit of induction motor with external capacitive reactance

The insertion of equal capacitors in each phase of the rotor circuit and the use of the space vector theory give the following equation set to model the dynamic behaviour of the WRIM [13] & [15]

$$U_s = R_s i_s + L_s di_s/dt + L_m di_r/dt \tag{1}$$

$$U_r = R_r i_r + L_r di_r/dt + L_m di_m/dt \tag{2}$$

$$du_{ce} = i_r^2 / c_e \tag{3}$$

$$T_e - T_1 = J dw_r/dt + D_w w_r \tag{4}$$

When the induction motor is operating under steady state condition i_s, i_r, U_{Cr} and r_w are constant. With a rotor capacitive reactance

circuit as supplementary supply in the rotor circuit, (1) and (2) become

$$U_s = R_s i_s + j\omega_1 L_s i_s + j\omega_1 L_m i_r \tag{5}$$

$$U_{ce} = R_r i_r + j\omega_2 L_r i_r + j\omega_2 L_m i_s \tag{6}$$

$$i_c = C_e du_{ce}/dt \tag{7}$$

Using equations (5) and (6) and the expression for apparent complex power is written

$$S = 3/2 U_s i_s S^* \tag{8}$$

From (8), formulae are deduced for the active and reactive power absorbed by the motor from the supply as a function of the motor parameters and the set load torque and they are

$$P = R_e(\bar{s}) = \frac{3}{2} |\sigma_s|^2 \frac{\left(R_r V_m - \omega_2 W_m \left(L_r - \frac{1}{\omega_2^2 C_e^2} \right) \right)}{V_m^2 + W_m^2} \tag{9}$$

$$Q = R_{im}(\bar{s}) = \frac{3}{2} |\sigma_s|^2 \frac{R_r W_m - \omega_2 V_m \left(L_r - \frac{1}{\omega_2^2 C_e^2} \right)}{V_m^2 + W_m^2} \tag{10}$$

Where,

$$V_m = R_s R_r + \omega_1 \omega_2 L_m^2 - \omega_1 \omega_2 L_s \left(L_r - \frac{1}{\omega_2^2 C_e^2} \right)$$

$$W_m = \omega_1 L_s R_r - \omega_2 R_s \left(L_r - \frac{1}{\omega_2^2 C_e^2} \right)$$

Thus, the power factor estimated from (9) and (10) is

$$\cos\phi = \frac{P}{\sqrt{P^2 + Q^2}} \tag{11}$$

3. PROPOSED ROTOR CAPACITIVE REACTANCE CONTROL SCHEME

In [14], the paper describes the switched capacitor concept which is used to improve the power factor of the inductive circuit. It consists of ac capacitor in the middle of an H bridge with bidirectional switches as shown in Fig.3 and Fig.4. The complementary switch pairs (S1, S4)

and (S2, S3), respectively, are switched using pulses generated using DSP controller.

During time interval, when the switch pair (S1, S4) is ON the capacitor is charging and a serial RLC circuit is modelled. In the time interval, when the switch pair (S2, S3) is ON the capacitor is applied with reverse polarity to the Rr-Lr circuit and the capacitor starts discharging. The time period is given by

3.1 Dynamic Capacitor concept:

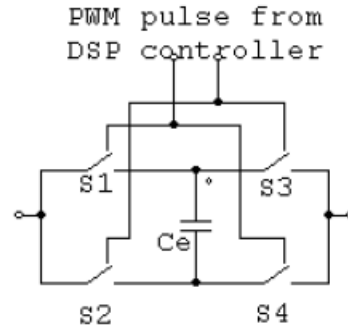


Figure 3. Basic H-Bridge switches with Capacitor

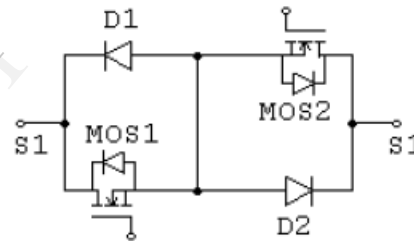


Figure 4. Bidirectional switch S1

$$T = T_{on} + T_{off} \tag{13}$$

$$d = \frac{T_{on}}{T} \tag{14}$$

In this way, the effective value of the rotor capacitance is given by

$$C_e = \frac{C}{(2d-1)^2} \tag{15}$$

The switched capacitor concept is adopted in the proposed method to change the capacitance value dynamically in the rotor circuit. The effective value of capacitance with respect to duty ratio for C=100µF is shown in Fig.5.

3.2 Theory of rotor capacitive reactance control:

In rotor capacitive reactance control, the rotor circuit is added with an external capacitive

reactance circuit in such that the rotor impedance is varied. By alteration of rotor impedance, the performance characteristics of the motor can be changed [6]-[11].

The secondary impedance/reactance control can be classified as rotor resonant control and non-resonant control schemes.

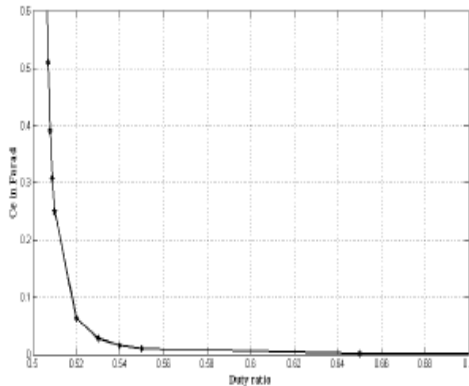


Figure 5. C_e Vs Duty ratio for $C=100\mu F$

3.2.1. Rotor resonant control:

In [12], the rotor circuit is operated by resonating at slip frequency by adding external rotor capacitive reactance which cancels the rotor inductive reactance. This method is effectively used for controlling the speed. This method has also shown improvement in power factor at about 5%. This technique has also proved large torque at starting and low speed conditions. The drawback of this method is large capacitance required to operate the rotor at resonant conditions and no control strategy has been adopted for speed - torque control and performance improvement. A fuzzy controller based rotor resonant control has been investigated for the performance enhancement WRIM in [18].

3.2.2. Non-Rotor resonant control:

In non-resonant control scheme, the rotor circuit is added with controllable capacitor in open loop mode. In this method, rotor capacitance value is varied in discrete steps in order to vary the secondary reactance value at different operating conditions. This method requires a large value of capacitance for control. In order to overcome the large capacitance requirement and avoiding the usage of discrete capacitance for control, dynamic capacitor concept has been suggested in each phase of the rotor circuit as described in [13] and [14]. In [13], a open loop control scheme by using

dynamic capacitor has been introduced for performance enhancement of WRIM. The drawbacks of this method were usage of more number of switches used in the three H-bridge circuits in the rotor circuit which in turn produces pulsating torque and time harmonics. The pulsating torque produced by this method has been described in [18].

In the proposed scheme which is a non-resonant control, only one H-bridge dynamic capacitor along with a bridge rectifier circuit shown in Fig.1 is employed. The rotor capacitance value is varied by varying the duty ratio of the dynamic capacitor.

3.2.3. Modes of Operation of Proposed scheme:

The switched capacitor is connected to the dc side of the rectifier. The rotor equivalent rotor resistance and reactance per phase is represented by R_r and L_r in series as shown in Fig.6. In Fig.1, the diodes are numbered according to the sequence in which they begin to conduct. Out of the diodes 1, 3 and 5 with common cathode connections, the diode connected to the highest positive phase voltage would conduct. Similarly, out of the diodes 2, 4 and 6, with common anode connections, the diode connected to the most negative phase voltage would conduct. If the three phase voltage waveforms are drawn and examined, it will be easily seen that the diodes conduct in the sequence 1,2,3...and so on. Each diode conducts for 120 degrees per cycle, and a new diode begins to conduct after a 60 degree interval. The output voltage waveform, V_c , which consists of portions of the line-to-line ac voltage waveforms, repeats with a 60 degree interval making it a six-pulse rectifier.

The per phase equivalent circuit of during conduction and non-conduction periods are shown in Fig.6. The H-bridge switched capacitor acts as filter well as a negative reactance voltage source control. The equivalent rectifier model of rotor circuit during conduction period is illustrated in Fig.5.

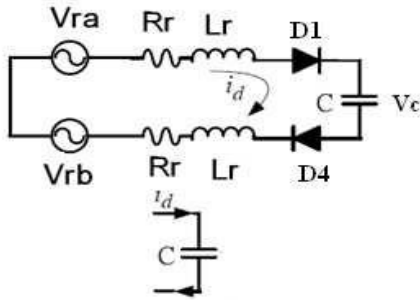


Fig.6. Rotor side Rectifier model during conduction

4. SIMULATION AND EXPERIMENTAL RESULTS

4.1 Hardware Implantation of Proposed Scheme:

A three phase wound rotor machine with rating and parameters shown in Table 1 (appendix) is used for experimental setup. The capacitor used for H-Bridge circuit was 100µF and the switching frequency was of 4 kHz. A TMS320F2407 Digital Signal Processor (DSP) controller was used for generating PWM pulses for appropriate switches.

The pulses from DSP are given to switches through opto-coupler which isolate the control circuit from power circuit. The pulses generated for duty ratio $d=0.55$ is shown in Fig.8. A power spectrum analyzer was used to measure the input active, reactive power, power factor, voltage, current, order of harmonics and monitoring the THD level. Initially the motor is run as squirrel cage induction motor and performance parameters are measured for different loading conditions.

4.1.1. Variable torque with constant emulated capacitor:

In the second instance, the tests were conducted for obtaining the power factor and efficiency, variation of speed at different loads with varying duty ratio. The measured readings are presented in Table 2 (appendix) and the performances of the motor are shown in Fig.9 (a) and 9 (b).

4.1.2. Constant torque with variable emulated capacitor:

In this case, the variation of power actor, efficiency, and speed as function of duty ratio at different load torque were analyzed. The

experimental results are presented in Table 3 (appendix) and the performance curves are shown in Fig.9 (c), and 9(d).

4.1.3. THD analysis:

The harmonics due to influence of rectifier circuit and switching were analyzed using power spectrum analyzer as function of load. In this case, the test results show that the higher order harmonics were very small at loaded conditions than no load condition. The experimental results for order of harmonics and THD level are shown in Fig.10 (a) for rotor shorted, Fig.10 (b) and Fig.(c) depict THD of different load conditions of proposed method. The voltage across capacitor and bridge rectifier voltage are presented at Fig.11 (a) and Fig.11 (b) respectively. The speed characteristics are shown in Fig.12.

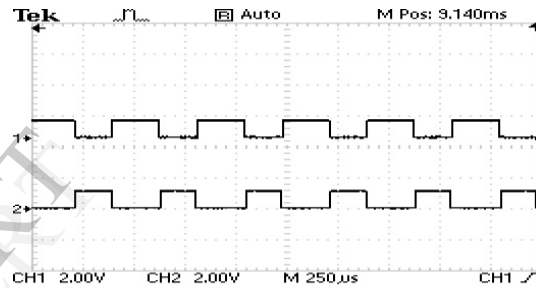
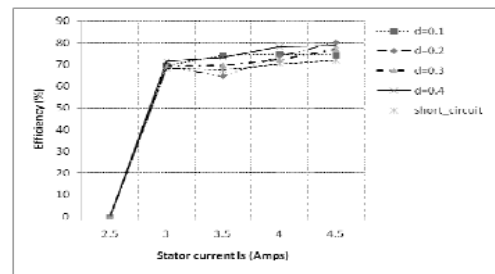
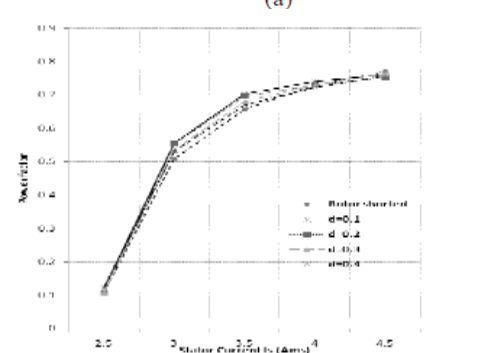


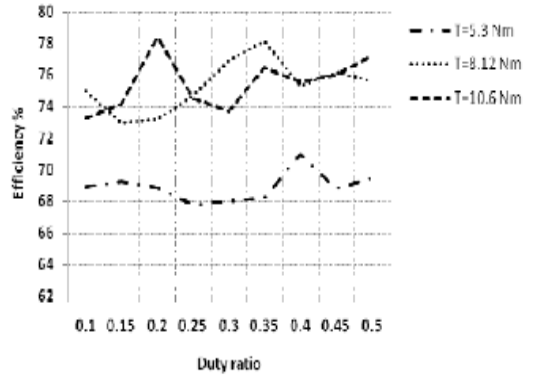
Fig. 8. Pulses for switched capacitor at $d=0.45$



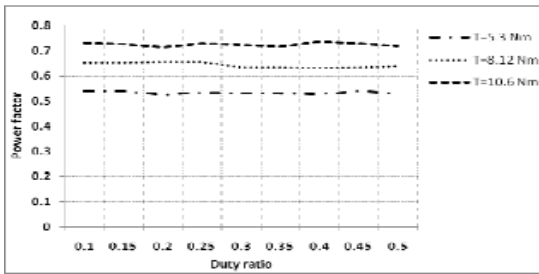
(a)



(b)

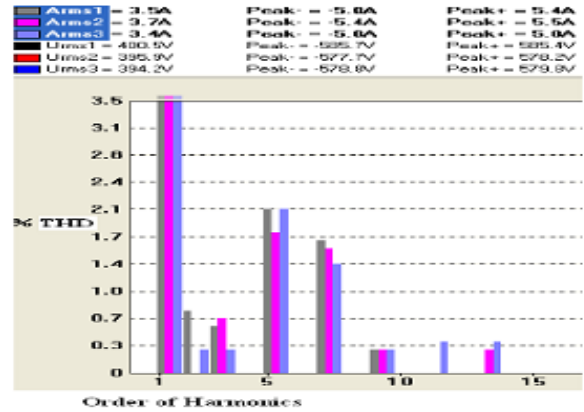


(c)



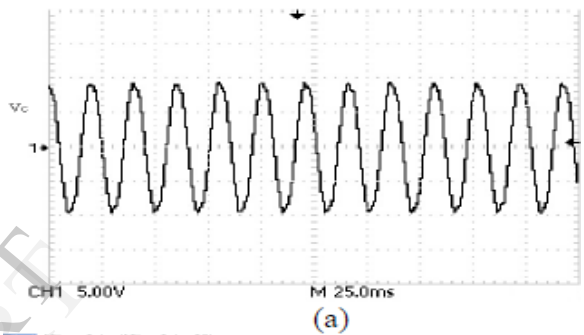
(d)

Fig.9. Experimental results: a.) Efficiency Vs Stator current b.) Power factor Vs Stator current (c) Efficiency Vs Duty ratio (d) Power factor Vs Duty ratio

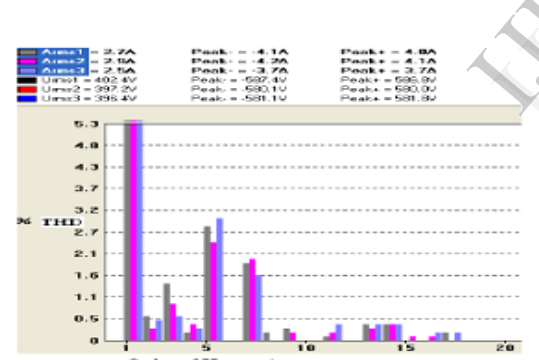


(c)

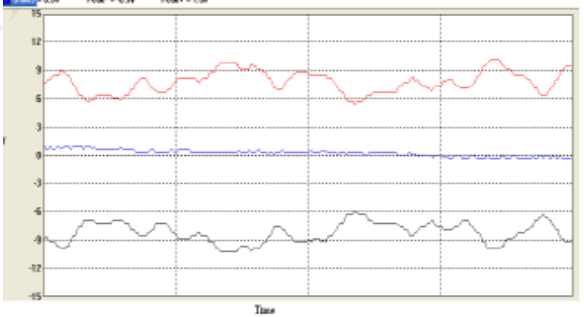
Fig.10. Experimental results : THD of Stator current at (a) rotor shorted (b) & (c) proposed scheme at different load



(a)

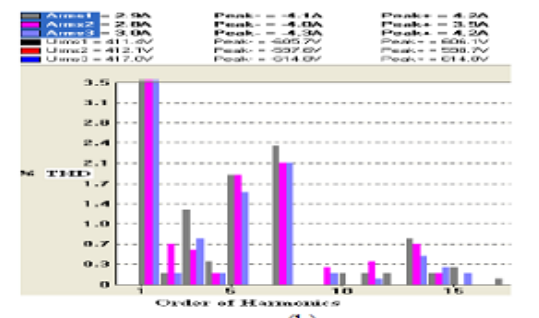


(a)



(b)

Fig.11.Voltage (a) Switched capacitor (b) Bridge rectifier



(b)

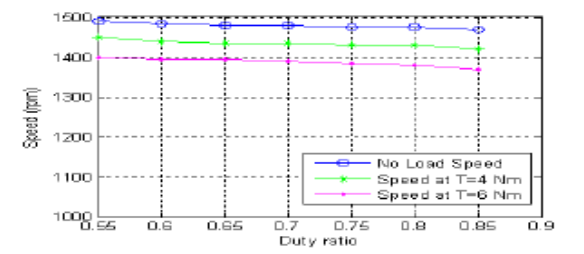
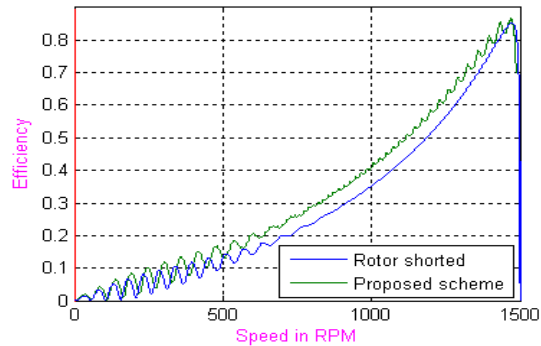


Fig.12.Speed Vs. Duty ratio

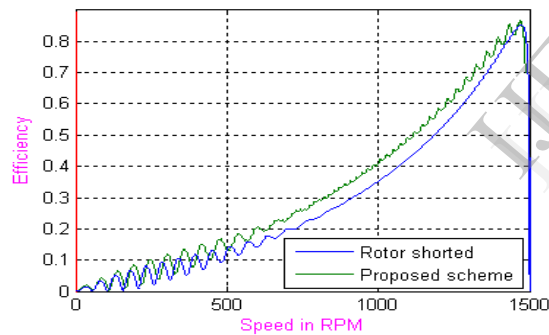
4.2. Simulation of Proposed scheme:

The three phase Induction motor for the same machine parameters were used for

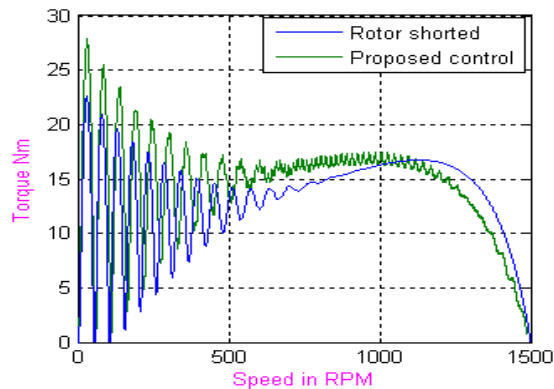
simulation using Matlab/Simulink. The performances such as Efficiency, power factor, speed and torque were studied. The simulation results are presented in Fig.13 (a), Fig.13(b) and Fig.13 (c). The performance is improved at starting and running. The starting torque is high compared with the results of short circuited operation of the motor. The torque ripples are minimum compared with the results presented in fuzzy controlled rotor capacitive reactance control [18].



(a)



(b)



(c)

Fig.13. Simulation results (a) Efficiency Vs speed (b) Power factor Vs Speed (c) Torque Vs Speed

4.3 Discussion

The experimental results with respect to proposed scheme are analyzed at different loadings and various emulated capacitor conditions. The proposed scheme at variable torque shows the efficiency improvement of up to 10% and the power factor improvement of 7% as illustrated in Fig.7(a) and Fig.7(b) respectively. These results show good agreement with simulation results as shown in Fig.10 (a) and Fig.10 (b). At constant torque instance, by varying the duty ratio of H-Bridge circuit, the emulated capacitor values are changed. In this case, the efficiency and power factor variations obtained are 15% and 8% respectively which is shown in Fig.7(c) and Fig.7(d). However, the speed variations are only 2% for different duty ratios. With the inclusion of Rx in the rotor circuit, the speed profile can be improved in wide range. The THD levels as a function of order of harmonics are analyzed when the rotor circuit employs bridge rectifier circuit and H-Bridge switches. In the proposed technique, higher order harmonics are present at light loads as in Fig. 8(b). However, these higher order harmonics are decreased to very small at loaded conditions as in Fig.8(c). In overall performance, as the rotor circuit along with the emulated capacitor acting as a series tuned filter, the % of THD is less as compared to the operation of rotor short circuited motor.

5. CONCLUSION

A novel dynamic rotor capacitive reactance control scheme with hardware implementation using DSP controller and the experimental results obtained were presented in this paper. Compared with conventional rotor impedance control, reduced number of switches has been used and hence the control strategy is very simple and easily realizable at low cost. The simulation results obtained were compared with experimental results which show good correlation between them. The higher order harmonics for the proposed scheme are very small under loaded conditions and torque ripples are also minimal compared with existing methods. The proposed technique can be used for speed control, high starting and running torque, ability to operate the motor with high efficiency and power factor. The future work should include the minimization of harmonics due to diode bridge rectifier and switching

circuits at all loading conditions. As a future work, a three phase controlled converter with expert system such as fuzzy closed loop control for controlling the dynamic capacitor in the rotor circuit can be tried for minimizing the torque ripple which in turn may improve the performances of the motor. A neural network for optimal efficiency and fast operation of motor can also be suggested.

REFERENCES

- [1]. M.Ray, A.K.Datta, "A variable speed induction motor using thyristor chopper", *Proceedings of IEEE, Vol. 62, n.10*, Nov. 1974, pp.1397-1397.
- [2]. P.C.Sen, K.H.J.Ma, "Rotor chopper for Induction motor Drive: TRC strategy", *IEEE Trans. On Industrial Applications, Vol. IA-11*, Jan./Feb., 1975, pp. 43-49.
- [3]. N.S.Wani, M.Ramamoorthy, "Chopper controlled slip ring induction motor", *IEEE Trans. on Industrial Electronics and Control Instrumentation, Vol. IECI-24, n.2*, June 1977, pp.153-161.
- [4]. P.C.Sen, K.H.J.Ma, "Constant Torque operation of Induction motors using chopper in rotor circuit", *IEEE Trans. on Industrial Applications, Vol. IA-14*, Sep./Oct. 1978, pp. 408-414.
- [5]. Chin S.Moo, Chung C.Wei, Ching L.Huang Chao S.Chen, "Starting control of Wound rotor induction motor by using chopper controlled Resistance in rotor circuit", *Proceedings of IEEE*, 1989, pp. 2295-2300.
- [6]. M.Ayyadurai, B.P.Singh, C.S.Jha, R.Arokiasamy, "On the speed control of wound rotor induction motor using rotor impedance control", *IEEE Trans. on Power Apparatus and systems, Vol.1, PAS-98, n.5*, Sep./Oct. 1979, pp. 1489-1496.
- [7]. W.Shepherd and G.R.Slemon, "Rotor impedance control of the wound rotor induction motor", *AIEE Trans., Pt III, Vol 78*, Oct 1959, pp 807-814.
- [8]. Y. Baghouz and O. T. Tan, "Optimal efficiency speed control of induction motors by variable rotor impedance," *IEEE Trans. Energy Conv.*, Vol. 4, June 1989, pp. 216-223.
- [9]. Dr. Saeed Ilesan, Dr. Mohamed S.Smiai, Prof. William shepherd, "Control of Wound Rotor Induction motor using thyristor in the secondary circuits," *IEEE Trans.*, 1993, pp.380-389.
- [10]. Dr.Saeed Ilesan, Prof. William shepherd, "Control of Wound Rotor Induction motor using rotor impedance variation," *Proc. Of IEEE Trans*

IAS Annual Meeting, Toronto Canada, Oct.1993, pp.2115-2122.

- [11]. H.Salama, M.Kansara, P.G.Holmes, Y.Safar, "Optimal Steady state performance of induction motor drives", in *Proc. Of OPTIM'96*, May 1996, pp- 1347-1360.
- [12]. J. Reinert and M. J. Parsley, "Controlling the speed of an induction motor by resonating the rotor circuit," *IEEE Trans. Ind. Applicat., Vol. 31*, July/Aug. 1995, pp. 887-891.
- [13]. Constantin Suciuc, Mohan Kansara, Peter Holmes, and Wilibald Szabo, "Performance Enhancement of an induction motor with secondary impedance control", *IEEE Transactions on Energy conversion, Vol 7, n.2*, 2002, pp. 211 - 216.
- [14]. C.Suciuc, M.Kansara, P.G.Holmes, W. Szabo, "Phase advancing for current in R-L circuits using switched capacitors", in *Electronics letters, Vol. 35, n.16*, Aug. 1999, pp-1296- 97.
- [15]. C.Suciuc, M.Kansara, P.G.Holmes, "A Space vector model of a static leading VAR secondary controlled induction machine", in *Proc. of OPTIM '98*, May 1998, pp- 375- 379.
- [16]. M.Y. Abdelfattah, "Speed control of wound rotor induction motors using chopper controlled external resistance enhanced with a dc capacitor", *Alexandria Engineering Journal, Vol. 42,n.1*, 2003, pp. 25-34.
- [17]. B.K.Bose, "Power Electronics and AC drives", (Englewood Cliffs, NJ: Prentice Hall, 1986).
- [18]. K.Ranjith kumar, S.Palaniswami, "Performance enhancement of Wound rotor induction motor by resonating rotor circuit using Fuzzy controller", *European Journal of Scientific Research, Vol.52, n.4*, 2011, pp. 580-591.
- [19]. E.S. Elwakil, M.K. Darwish, "Critical Review of converter topologies for Switched Reluctance Motor Drives", *International Review of Electrical Engineering (IREE)*, vol. 2, n.1, Jan.- Feb. 2007, pp. 50 - 58.

Nomenclature

\bar{U}_r	Space phasor of rotor voltage
\bar{U}_s	Space phasor of stator voltage
\bar{U}_{ce}	Space phasor of rotor capacitive voltage
R_s	Stator resistance per phase
R_r	Rotor resistance per phase
L_s	Stator self inductance per phase
L_r	Rotor self inductance per phase
C_e	Rotor effective capacitance (Value of dynamic capacitance value)
X_{L_r}	Rotor inductive reactance
X_{C_e}	Rotor capacitive reactance
\bar{i}_s	Space phasor of stator current
\bar{i}_r	Space phasor of rotor current
ω_1	Angular velocity from the stator circuit
ω_2	Angular velocity from rotor circuit
ω_r	Angular speed of rotor circuit
D_w	Damping factor
J	Moment of Inertia
P, Q	Active power and reactive power
$\cos\phi$	Power factor
\bar{S}	Apparent complex power
P	Pole pairs
C_e	Effective rotor capacitance value
C	Capacitance in the H-Bridge circuit
d	Duty ratio of the H-bridge switch

APPENDIX

Table 1. Specifications for Simulation and experiment

Components	Part name/ Manufacturer	Rating values
P, V	Motor rating (Power, Voltage)	2.2kW - 415V
f, p	(frequency, Poles)	50Hz - 4
R_s	Stator resistance	5.6 Ω
R_r	Rotor resistance	2.22 Ω
L_s, L_r	Stator and rotor inductance	12.7 mH
L_m	Mutual inductance	291 mH

Table 2. Measured readings for rotor short circuit

I_s (A)	Input Power(W)	Output power(W)	Speed (RPM)	Torque (Nm)	Effi. (%)	Power factor
Rotor short circuit						
2.5	207.6	0	1420	0	0	0.108
3	1130.87	740.52	1390	5.07	65.53	0.508
3.5	1725	1131.37	1370	7.89	65.56	0.657
4	2132.3	1434.2	1350	10.15	67.26	0.728
4.5	2491.9	1791.93	1320	12.97	71.9	0.77

Table 3. Measured readings for constant duty ratio

I_s (A)	Input Power(W)	Output power(W)	Speed (RPM)	Torque (Nm)	Effi. (%)	Power factor
Rotor short circuit						
2.5	207.6	0	1420	0	0	0.108
3	1130.87	771	1390	5.3	68.23	0.508
3.5	1725	1164.35	1370	8.12	67.5	0.657
4	2132.3	1497.78	1350	10.6	70.25	0.728
4.5	2491.9	1791.93	1320	12.97	71.9	0.77
DUTY RATIO=0.1						
2.5	181.9	0	1410	0	0	0.12
3	1109.01	771	1390	5.3	69.52	0.556
3.5	1571.8	1164.35	1370	8.12	74.07	0.703
4	1984.3	1486.57	1340	10.6	74.93	0.74
4.5	2412	1791.93	1320	12.97	74.3	0.76
DUTY RATIO=0.2						
2.5	183.8	0	1420	0	0	0.106
3	1112.5	765.5	1380	5.3	68.83	0.553
3.5	1792.4	1155.85	1360	8.12	64.5	0.6963
4	2030.9	1497.2	1350	10.6	73.74	0.73
4.5	2256.9	1805.5	1330	12.97	80.05	0.753
DUTY RATIO=0.3						
2.5	185.4	0	1430	0	0	0.108
3	1122.2	776.6	1400	5.3	69.21	0.535
3.5	1686.7	1172.85	1380	8.12	69.53	0.68
4	2108.95	1520	1370	10.6	72.1	0.73
4.5	2360.7	1819	1340	12.97	77.07	0.763
DUTY RATIO=0.4						
2.5	212.3	0	1420	0	0	0.123
3	1079	771	1390	5.3	71.45	0.531
3.5	1587.7	1164.35	1370	8.12	73.4	0.669
4	1918.6	1497.7	1350	10.6	78.05	0.723
4.5	2277.7	1791.93	1320	12.97	78.66	0.757

Table 4. Measured readings for constant load Torque

Duty Ratio (d)	Speed (rpm)	Input Power (W)	Output Power (W)	Efficiency (%)	Power factor
Load Torque $T_L=5.3$ Nm ($I_s=3A$)					
0.1	1390	1119	771	68.9	0.54
0.15	1350	1119.5	774.89	69.25	0.539
0.2	1360	1097	754.43	68.88	0.524
0.25	1370	1121.5	759.98	67.8	0.533
0.3	1340	1093.8	743.34	68	0.531
0.35	1360	1105.2	754.43	68.23	0.53
0.4	1390	1086.2	771	71	0.528
0.45	1370	1105.2	759.98	68.8	0.538
0.5	1380	1102.2	765.5	69.5	0.53
Load Torque $T_L=8.1$ Nm ($I_s=3.5A$)					
0.1	1350	1530.48	1147.3	74.96	0.652
0.15	1330	1547.43	1130.3	73	0.653
0.2	1350	1567.61	1147.35	73.2	0.654
0.25	1360	1547.73	1155.85	74.7	0.655
0.3	1370	1513	1164.35	76.93	0.633
0.35	1380	1502	1172.85	78.1	0.634
0.4	1350	1522.9	1147.35	75.3	0.631
0.45	1360	1517.5	1155.85	76.2	0.634
0.5	1340	1507.8	1138.85	75.6	0.639
Load Torque $T_L=10.6$ Nm ($I_s=4 A$)					
0.1	1350	2045.9	1497.78	73.25	0.731
0.15	1340	1978.38	1486.68	74.16	0.725
0.2	1350	1911.25	1497.78	78.38	0.714
0.25	1330	1980.9	1475.6	74.54	0.727
0.3	1310	1970.3	1453.4	73.75	0.724
0.35	1320	1915.8	1446.5	76.45	0.717
0.4	1330	1952.32	1457.6	75.56	0.734
0.45	1340	1957.34	1486.68	75.98	0.729
0.5	1330	1962.98	1475.6	77.2	0.719